IN-39
136227
P.16

NASA Technical Memorandum 105779

Root Damage Analysis of Aircraft Engine Blade Subject to Ice Impact

E.S. Reddy and G.H. Abumeri
Sverdrup Technology, Inc.
Lewis Research Center Group
Brook Park, Ohio

and

C.C. Chamis and P.L.N. Murthy
National Aeronautics and Space Administration
Lewis Research Center
Cleveland, Ohio

August 1992

NASA

TABLE OF CONTENTS

LIST OF SYMBOLS

E	Young's modulus
F_r	generalized force on r^{th} mode
$\hat{F}_r$	impulse on (or initial velocity of) r^{th} mode
$\{f\}$	force vector
$\hat{f}_j$	impulse on j^{th} mode
G	Shear Modulus
g	defined by Equation (14)
$[K]$	generalized stiffness matrix
$[k]$	stiffness matrix
$[M]$	generalized mass matrix
M_r	generalized mass for r^{th} mode
$[m]$	mass matrix
N	number of modes considered in the response computation
n	total number of degrees of freedom
$\{q\}$	vector of n degrees of freedom
$\{\ddot{q}\}$	acceleration vector for n degrees of freedom
S_{11}, S_{22}, S_{12}	strength of the material in 11, 22 and 12 direction
t	time
$\{u\}$	modal vector of n degrees of freedom
$[u]$	modal matrix
$\{\ddot{u}\}$	modal acceleration vector of n degrees of freedom
$\gamma_{12\beta}$	defined by Equation (15)
$\{\eta\}$	modal coordinate vector
$\{\ddot{\eta}\}$	modal acceleration vector
ν_{12}, ν_{13}, ν_{21}, ν_{23}	Poisson's ratios
σ_{11}, σ_{22}, σ_{12}	induced stresses in 11, 22 and 12 directions

$\{\hat{\sigma}\}^i$	element stress vector corresponding to i^{th} mode shape
$\{\sigma\}$	element stress vector
ω_r	r^{th} natural frequency
$[\omega^2]$	diagonal matrix of natural frequencies

ROOT DAMAGE ANALYSIS OF AIRCRAFT ENGINE BLADE SUBJECT TO ICE IMPACT

E. S. Reddy and G. H. Abumeri
Sverdrup Technology, Inc.
Lewis Research Center Group
Brook Park OH 44142

C. C. Chamis and P. L. N. Murthy
NASA Lewis Research Center
Cleveland OH 44135

ABSTRACT

The blade root response due to ice impact on an engine blade is simulated using the NASA in-house code *BLASIM*. The ice piece is modeled as an equivalent spherical object impacting on the leading edge of the blade and has the velocity opposite to that of the aircraft with direction parallel to the engine axis. The effect of ice impact is considered to be an impulse load on the blade with its amplitude computed based on the momentum transfer principle. The blade response due to the impact is carried out by modal superposition using the first three modes. The maximum dynamic stresses at the blade root are computed at the quarter cycle of the first natural frequency. A combined stress failure function based on modified distortion energy is used to study the spanwise bending damage response at the blade root. The damage function reaches maximum value for very low ice speeds and increases steeply with increases in engine speed.

INTRODUCTION

At high altitudes, when aircraft flies through clouds of super-cooled water droplets, ice formation occurs on forward facing structural components. One such component is the engine inlet. With time, the ice accretes on the inlet and eventually sheds due to structural vibrations. As a result, blocks of ice travelling at the speed of aircraft impacts the engine blades rotating at high RPM. A schematic of this phenomenon is shown in Figure 1. This process may cause severe damage at the blade root and subsequently may result in catastrophic failure of the engine.

In this paper, the blade root response due to ice impact on an engine blade is simulated using the NASA in-house code *BLASIM* [1]. The ice piece is modeled as an equivalent spherical object impacting on the leading edge of the blade. The ice piece velocity is opposite to that of the aircraft with direction parallel to the engine axis. The effect of ice impact is considered to be same as that caused by an impulse load on the leading edge of the blade with an equivalent amplitude computed based on the momentum transfer principle. The dynamic analysis is carried out by finite element method andthe blade response due to this impact is carried out by modal superposition. However, experience has shown that the highest root stresses occur at the quarter cycle of the first bending frequency [2]. A combined stress failure function based on modified distortion energy [3] is then used as a measure of the root damage response due to impact. The details of the linear response analysis as implemented in the code are presented. The root damage response capability of the code is demonstrated by considering a modified SR-2 unswept propfan blade made. Parametric studies are performed and the effects of ice speed, ice size, engine speed and impact location on the root damage response are discussed.

ANALYSIS

Ice Impact Model

The geometry of ice impact on the leading edge of the blade is shown in Figures 2(a,b). The ice piece is modeled as an equivalent spherical object impacting on the leading edge of the blade. The impact on the blade arises from the momentum of the ice piece. The duration of impact is considerably short and for the purpose of obtaining the response at the root, the impact is considered as an impulse on a single node along the leading edge of the blade. Also, the impulse component normal to the chord, being the primary factor in causing the spanwise bending damage, is included in the response computation. The impact velocity direction relative to the blade is a function of the aircraft speed and the rotational speed of the blade (Figure 2a). The resulting impact depends on the magnitude and direction of the relative velocity and the mass of ice piece. Depending on the spacing (i.e., number) of blades and relative velocity, the ice piece that is approaching the blade under consideration is sheared off by the adjacent blade as shown in Figure 2b. As a result, only a portion of ice piece impacts the leading edge of the blade. Effectively, the size of the ice piece that finally impacts the blade depends on the blade spacing, blade speed and aircraft speed. The shape of the ice is considered to be a sphere only for simplicity and affects the determination of sheared part of the ice. Once the initial velocity equivalent to the impulse is computed, the remaining analysis does not depend on the ice shape.

Blade Finite Element Model

In the code, the blade geometry is input in the form of finite element grid and nodal thicknesses. The blade is modeled using three node triangular plate finite elements with six degrees of freedom per node. This finite element is similar to NASTRAN (TRIA3) [4,5]. The blade finite element mesh consists of 55 nodes and 80 elements. The planform of the blade considered for analysis and the corresponding finite element blade mode are shown in Figures 3a and 3b.

Response Analysis

The blade root response analysis, as implemented in the code is presented here. The governing equations of motion for an undamped discrete system of order n is given by

$$[m]\{\ddot{q}\} + [k]\{q\} = \{f\} \tag{1}$$

where $[m]$ is the mass matrix, $[k]$ is the stiffness matrix, $\{q\}$ is the vector of n degrees of freedom and $\{f\}$ is the forcing function.

Consider the first N modes ($N \leq n$) and let $[u]$ be the modal matrix of the above undamped system with N eigenvectors as its columns, i.e.,

$$[u] = [\{u\}^1, \{u\}^2, \cdots \{u\}^N] \tag{2}$$

and

$$\{q\} = [u]\{\eta(t)\} \tag{3}$$

then Equation (1) transforms to

$$[M]\{\ddot{\eta}\} + [K]\{\eta\} = [u]^T\{f\} \tag{4}$$

where $[M]$ and $[K]$ are the generalized mass and stiffness matrices, η and $\ddot{\eta}$ are the generalized coorduinate and the associated acceleration vectors.
The matrices $[M]$ and $[K]$ are diagonal due to orthogonal property of the modal matrix $[u]$.

Premultipling the Equation (4) by $[M]^{-1}$,

$$\{\ddot{\eta}\} + [\omega^2]\{\eta\} = [M]^{-1}[u]^T\{f\} \tag{5}$$

where ω's are the natural frequencies of the system and $[\omega^2] = [M]^{-1}[K]$.
Since the matrix Equation (5) is uncoupled, it can be written as

$$\ddot{\eta}_r(t) + \omega_r^2\eta_r(t) = \frac{1}{M_r}\sum_{i=1}^{n} u_i^r f_i(t), \quad r = 1,..N \tag{6}$$

where u_i^r is the i^{th} component of the r^{th} eigenvector and M_r is the generalized mass for the r^{th} mode. If the forcing function is acting only on one of the degrees of freedom, say $i=j$, then the Equation (6) simplifies to

$$\ddot{\eta}_r(t) + \omega_r^2\eta_r(t) = F_r(t), \quad r = 1,.. N \tag{7}$$

where $F_r(t) = \frac{u_j^r}{M_r} f_j(t)$

Instead of the forcing function, $F_r(t)$, if an impulse acts on the r^{th} generalized degree of freedom, the set of equations can be solved by applying an initial velocity condition. i.e.,

$$\ddot{\eta}_r(t) + \omega_r^2\eta_r(t) = 0, (r = 1,..n) \text{ with } \dot{\eta}_r(0) = \hat{F}_r \tag{8}$$

where $\hat{F}_r = \frac{u_j^r}{M_r}\hat{f}_j$ and $\hat{f}_j$ is the magnitude of impulse on j^{th} degree of freedom.
The solution of equation (8) can be written as

$$\eta_r(t) = \frac{u_j^r}{M_r\omega_r}\hat{f}_j \sin\omega_r t, (r = 1,..N) \tag{9}$$

Now, using the relation $\{q\} = [u]\{\eta(t)\}$, the nodal displacement response can be obtained as

$$q_i(t) = \sum_{r=1}^{N} u_i^r\eta_r(t) = \sum_{r=1}^{N} u_i^r\frac{u_j^r}{M_r\omega_r}\hat{f}_j \sin\omega_r t, (i=1,..n) \tag{10}$$

The q's can also be expressed in the form

$$\{q\} = \eta_1(t)\{u\}^1 + \eta_2(t)\{u\}^2 + \eta_3(t)\{u\}^3 + ... + \eta_N(t)\{u\}^N \tag{11}$$

If $\{\hat{\sigma}\}^i$ is the element stress vector that correspond to the mode shape $\{u\}^i$, then total stress response, $\{\sigma\}$ can be written as

$$\{\sigma(t)\} = \eta_1(t)\{\hat{\sigma}\}^1 + \eta_2(t)\{\hat{\sigma}\}^2 + \eta_3(t)\{\hat{\sigma}\}^3 + ... + \eta_N(t)\{\hat{\sigma}\}^N \tag{12}$$

The response of the blade due to impact (impulse loading) is expected to be predominantly first mode and hence the maximum stress occurs at or near the quarter cycle of the first mode frequency [2]. The stress vector at time, $t = \pi/2\omega_1$ is

$$\{\sigma(\frac{\pi}{2\omega_1})\} = \sum_{i=1}^{N} \eta_i(\frac{\pi}{2\omega_1})\{\hat{\sigma}\}^i \tag{13}$$

Computation of the Root Damage

The BLASIM code is capable of analyzing metallic as well as composite blades. In order to account for the complex loads and microscopic failure mechanisms, a combined stress function based on the modified distortion energy [3] is used as a measure of the blade failure. The general expression for a composite ply, g, is given by

$$g = \left(\frac{\sigma_{11\alpha}}{S_{11\alpha}}\right)^2 + \left(\frac{\sigma_{22\beta}}{S_{22\beta}}\right)^2 - \gamma_{12\beta}\frac{\sigma_{11\alpha}\sigma_{22\beta}}{S_{11\alpha}S_{22\beta}} + \left(\frac{\sigma_{12}}{S_{12}}\right)^2 \tag{14}$$

where $\alpha = \begin{cases} T \text{ (for tension) if } \sigma_{11} \geq 0 \\ C \text{ (for compression) if } \sigma_{11} < 0 \end{cases}$, $\beta = \begin{cases} T \text{ (for tension) if } \sigma_{22} \geq 0 \\ C \text{ (for compression) if } \sigma_{22} < 0 \end{cases}$

$$\gamma_{12\beta} = \gamma'_{12\beta}\frac{(1 + 4\nu_{12} - \nu_{13})E_{22} + (1 - \nu_{23})E_{11}}{[E_{11}E_{22}(2 + \nu_{12} + \nu_{13})(2 + \nu_{21} + \nu_{23})]^{1/2}} \tag{15}$$

S is the strength, E is modulus of elasticity, and ν is Poisson's ratio with subscripts 1 and 2 referring to the longitudinal and transverse directions of the fiber in a ply.

It is assumed that $\gamma'_{12\beta} = 1.0$ and $\nu_{23} = 1.25\nu_{12}$ in implementing the above equation in the code as these are typical values for a normal fiber composite system. The values of g are computed for all the elements (second row) at the blade root and the maximum is presented as a measure of blade root damage in this paper. Material is considered failed when the function value is equal to or greater than unity.

RESULTS AND DISCUSSION

The SR2 model unswept titanium blade [7] is considered to study the effect of ice impact on the root damage as shown in Figure 3a. The corresponding discretized finite element model is shown in Figure 3b. The setting angle (orientation of the blade chord with respect to the plane of rotation at 75% span) is 57° and the number of blades are eight. The titanium properties used in the numerical computation are: $E = 16.5\text{x}10^6\,psi$, $G = 6.4\text{x}10^6\,psi$, $\nu = 0.3$, $\rho = 0.00044\ lbf.sec^2/in^2$, $S_{11} = 7.4\text{x}10^4\,psi$, $S_{22} = 7.4\text{x}10^4\,psi$, $S_{12} = 4.4\text{x}10^4\,psi$, The range of engine speed is 500 - 10000 RPM and the maximum ice radius considered is 0.8".

The dynamic deformation shape of the blade is expected to be a simple one because of an impulse load at a point. Hence, the response computation through modal superposition technique is carried

out using first three modes. The midplane of the 3-D blade and the first three mode shapes (first bending, second bending and first torsion) are shown in Figures 4(a-d). In order to have a better 3-D visual effect, nodal data is interpolated and a dense mesh is shown in these Figures.

Effect of Ice Size and Speed.

The effects of ice size and ice speed at 3000, 5000 and 8000 RPM on the failure function are shown in Figures 5(a-c). The root damage is maximum when the ice size is maximum at all the engine speeds as expected. However, for a specified ice size, the damage reaches a maximum at relatively low ice speeds and thereafter decreases continuously. The optimum ice speeds that results in maximum root damage for the three engine speeds are 20, 30 and 40 knots respectively. The corresponding failure function values are 0.026, 0.076 and 1.22. This behavior is due to the fact that only the impulse component normal to the blade chord is considered to cause the spanwise bending damage. At a given engine speed, the impact relative velocity on the blade increases with increase in ice speed. As a result, the impulse on the blade increases but the impulse component normal to the blade chord decreases due to decrease in the impact angle relative to the chord, θ, as shown in Figure 6. For larger ice speeds, the value of θ gradually reduces to zero (see also Figure 2a).

Effect of Engine Speed

Figures 7 and 8 show the effect of engine speed on the root damage. The graphs shown are for an ice size of 0.8" radius and the impact location at 73.5% span along the leading edge. It can be seen from Figure 7 that the failure function increases steeply for larger values of engine speed (5000 - 8500 RPM) In the speed range approximately 8500 - 9000 RPM, it decreases steeply. The damage function, as expressed by the Equation (15) is a function of combined stresses due to centrifugal loading and impulse loading. Furthermore, centrifugal loading is $\sim \Omega^2$ and hence contributes to the damage more at higher values than that due to impulse.

The steep decrease can be attributed to the shearing action of the neighboring blade due to its proximity. In the absence of shearing action, the ice mass remains constant and impulse increases linearly with engine speed as shown by dashed line (Figure 8). However, due to shearing, the impacting mass of the ice and consequently the impulse reduces as shown by solid line. The ice, as the engine speed increases, start getting sheared off at approximately 5800 RPM by the adjacent blade (see Figure 2b).

Effect of Ice Impact Location

The impacting location of the ice is varied from approximately 30% to 75% of the blade span to study its effect on the root damage. Figure 9 shows that the relationship between the magnitude of root damage and the impact location is almost linear and the slope of the line depends upon the engine speed. As discussed in the previous section, the engine speed has a strong effect on the root response and hence the slope of the line for higher engine speeds is higher. For example, at 8000 RPM, the failure function has a value of 0.33 at 30% span and increases to 1.00 at 75% span.

CONCLUSIONS

The response at the root of an SR2 titanium blade due to ice impact is simulated via modal superposition technique. The failure function based on Modified Distortion Energy criteria is used as a measure of root damage. The following conclusions can be drawn from the results presented here:

1. The blade root damage due to spanwise bending increases with the increase in ice size and is maximum for low values of ice speeds.

2. At engine speed larger compared to ice speed (aircraft speed), ice piece gets sheared off resulting in lower impact mass and consequently low impulse on the blade. In effect, root damage is lower when shearing process takes place.

3. The engine speed has a stronger effect on the blade root damage especially at higher RPM (> 5000). This is due to the fact centrifugal loading is ~ Ω^2 and hence contributes more towards the root damage.

4. The root damage increases linearly with the increase in impact radius along the blade and the slope of the line is very high at larger engine speeds.

REFERENCES

1. Reddy, E. S.; Abumeri, G. H.: Blade Assessment for Ice Impact (BLASIM), User's Manual. NASA CR to be published.

2. Brown, K. W: Structural Tailoring of Engine Blades (STAEBL), Theoretical Manual. NASA CR 175112, 1985.

3. Murthy, P. L. N; and Chamis, C. C.: Integrated Composite Analyzer (ICAN). NASA TP 2515, 1986.

4. MacNeal, R. H.: A Simple Quadrilateral Shell Element. Computers and Structures, vol. 8, Pergamon Press, Great Britain, 1978, pp. 175-183.

5. MSC/NASTRAN, Version 65C, User's Manual. The MacNeal-Schwendler Corporation, 1987.

6. Thomson, W. T: Theory of Vibration with Applications. Prentice Hall, Inc., Englewood Cliffs, New Jersey, 1981.

7. Reddy, T. S. R.; and Kaza, K. R. V.: Analysis of an Unswept Propfan Blade With a Semiempirical Dynamic Stall Model. NASA TM 4083, 1989.

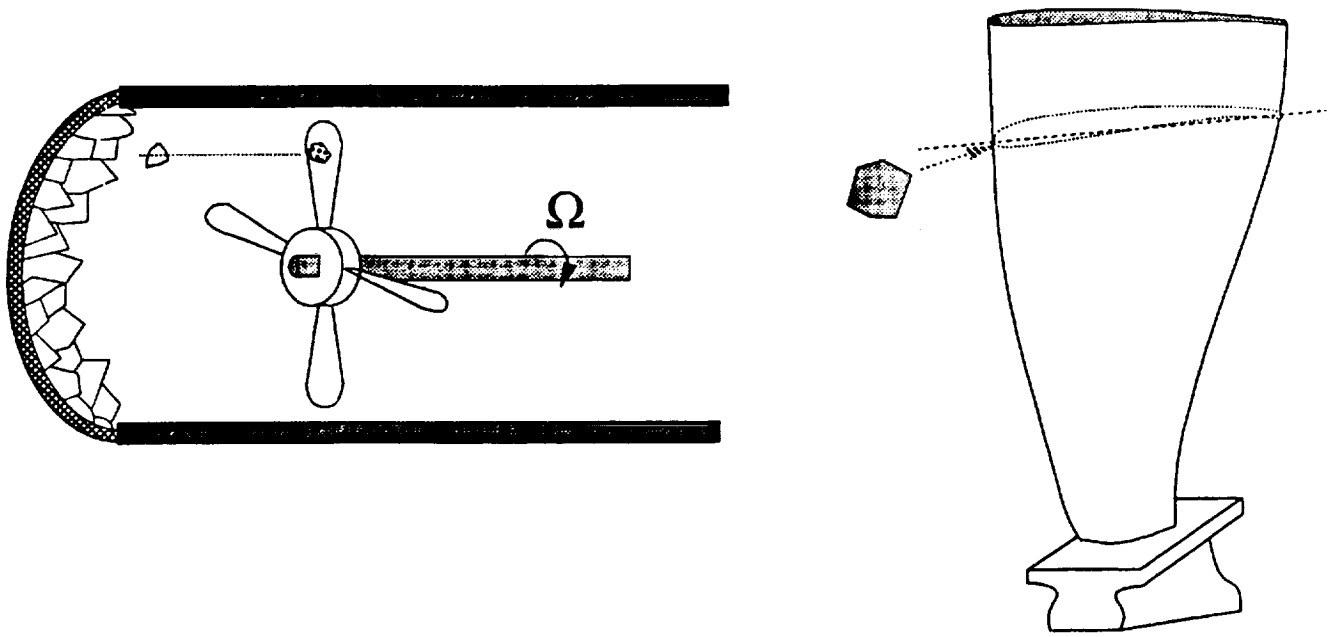

Figure 1.—A schematic of ice impact on an engine blade.

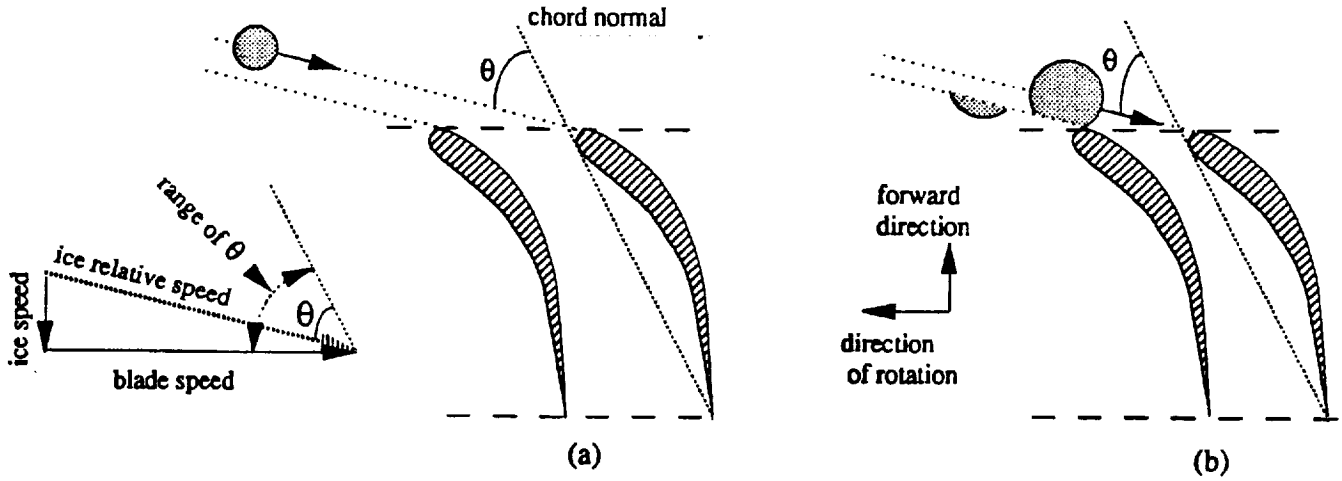

Figure 2.—Geometry of ice impact on an engine blade.

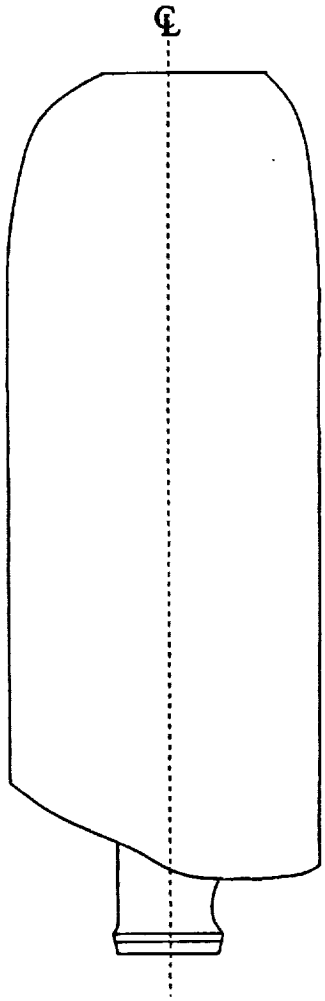

(a) Planform of SR-2 model propfan blade.

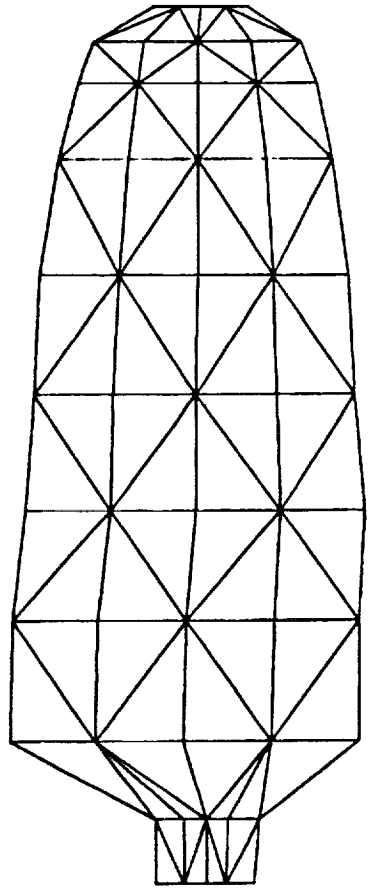

(b) Blade finite element model.

Figure 3.

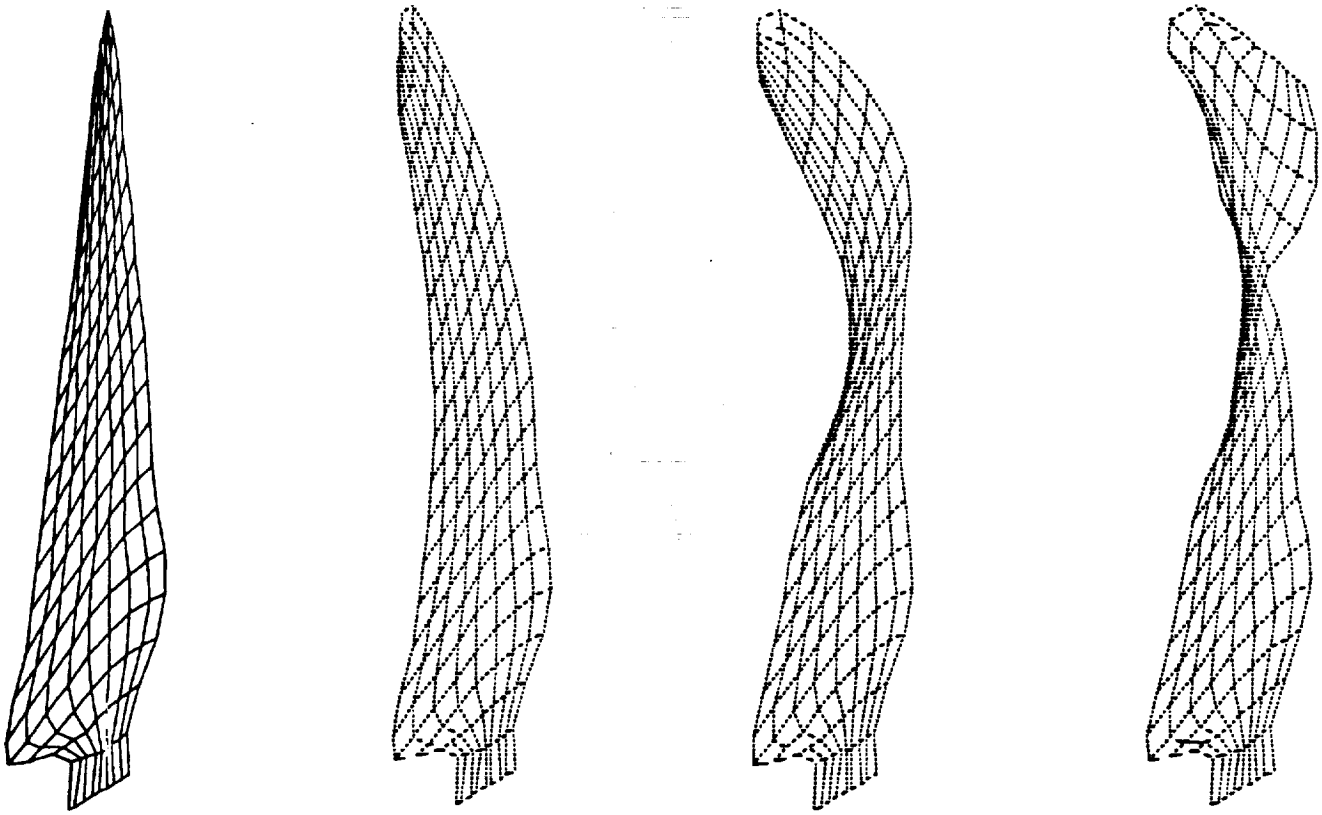

Figure 4.—SR2 blade and the first three mode shapes.

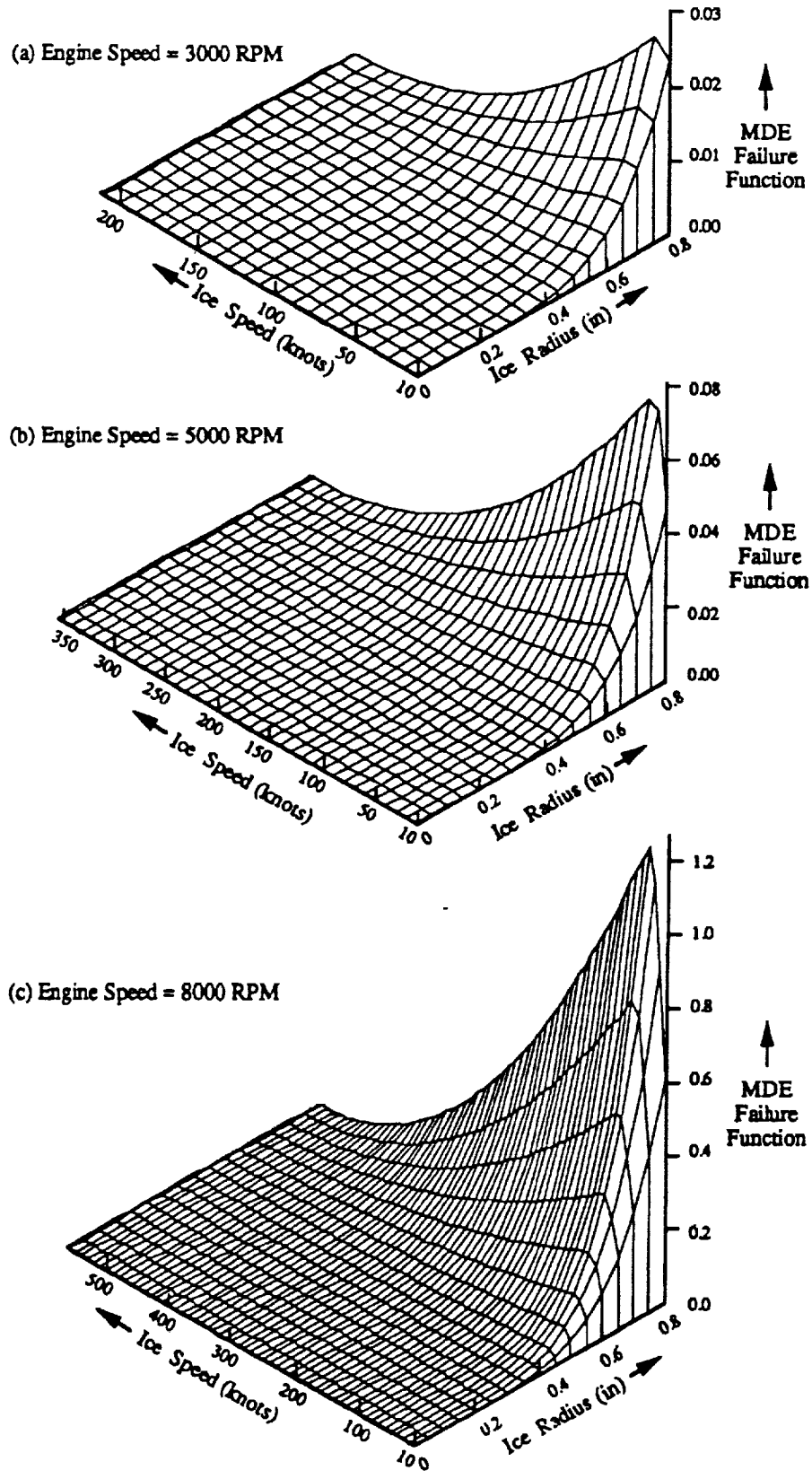

Figure 5.—Effect of ice radius and ice speed on blade root damage.

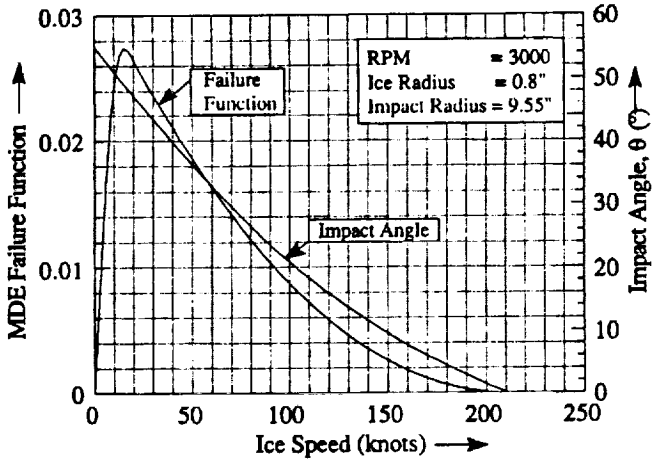

Figure 6.—Effect of ice speed on blade root damage and impact angle.

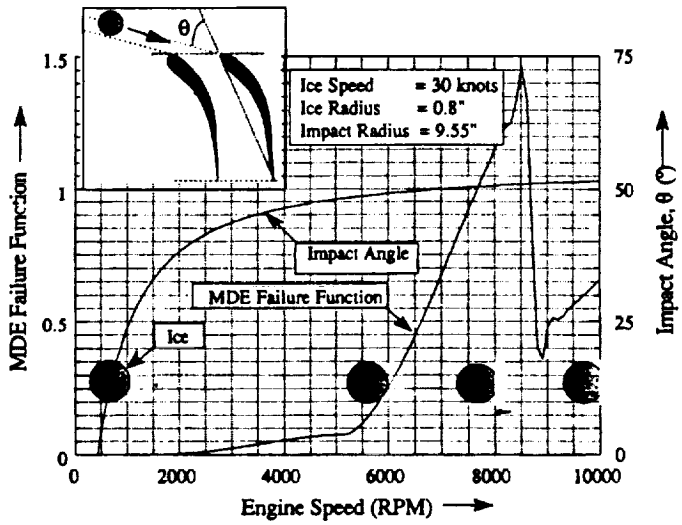

Figure 7.—Effect of engine speed on blade root damage.

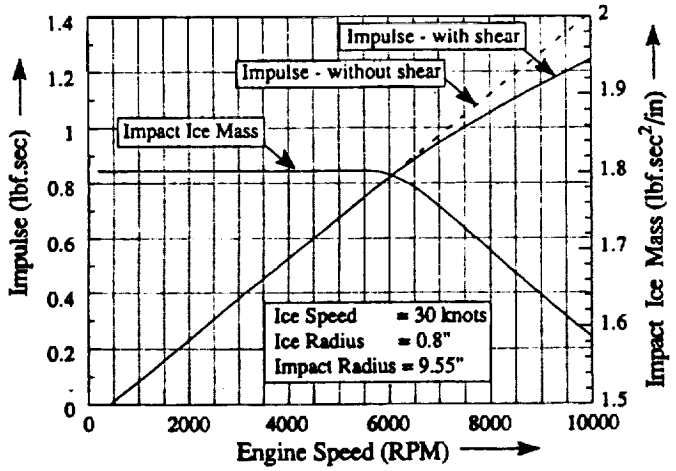

Figure 8.—Effect of engine speed on impulse and impacting ice mass.

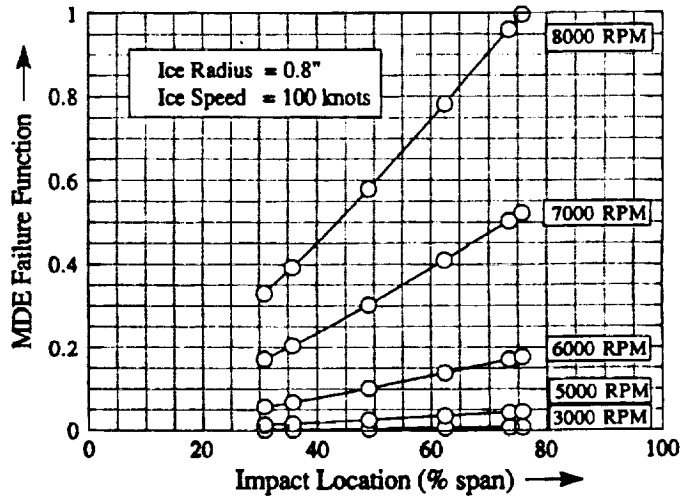

Figure 9.—Effect of ice impact location on blade root damage.

REPORT DOCUMENTATION PAGE

Form Approved
OMB No. 0704-0188

1. AGENCY USE ONLY (*Leave blank*)	2. REPORT DATE	3. REPORT TYPE AND DATES COVERED
	August 1992	Technical Memorandum

4. TITLE AND SUBTITLE

Root Damage Analysis of Aircraft Engine Blade Subject to Ice Impact

5. FUNDING NUMBERS

WU-505-62-0K

6. AUTHOR(S)

E.S. Reddy, G.H. Abumeri, C.C. Chamis, and P.L.N. Murthy

7. PERFORMING ORGANIZATION NAME(S) AND ADDRESS(ES)

National Aeronautics and Space Administration
Lewis Research Center
Cleveland, Ohio 44135-3191

8. PERFORMING ORGANIZATION REPORT NUMBER

E-7206

9. SPONSORING/MONITORING AGENCY NAMES(S) AND ADDRESS(ES)

National Aeronautics and Space Administration
Washington, D.C. 20546-0001

10. SPONSORING/MONITORING AGENCY REPORT NUMBER

NASA TM-105779

11. SUPPLEMENTARY NOTES

E.S. Reddy and G.H. Abumeri, Sverdrup Technology, Inc., Lewis Research Center Group, 2001 Aerospace Parkway, Brook Park, Ohio 44142. C.C. Chamis and P.L.N. Murthy, NASA Lewis Research Center, Cleveland, Ohio. Responsible person, P.L.N. Murthy, (216) 433-3332.

12a. DISTRIBUTION/AVAILABILITY STATEMENT

Unclassified - Unlimited
Subject Category 39

12b. DISTRIBUTION CODE

13. ABSTRACT (*Maximum 200 words*)

The blade root response due to ice impact on an engine blade is simulated using the NASA in-house code *BLASIM*. The ice piece is modeled as an equivalent spherical object impacting on the leading edge of the blade and has the velocity opposite to that of the aircraft with direction parallel to the engine axis. The effect of ice impact is considered to be an impulse load on the blade with its amplitude computed based on the momentum transfer principle. The blade response due to the impact is carried out by modal superposition using the first three modes. The maximum dynamic stresses at the blade root are computed at the quarter cycle of the first natural frequency. A combined stress failure function based on modified distortion energy is used to study the spanwise bending damage response at the blade root. That damage function reaches maximum value for very low ice speeds and increases steeply with increases in engine speed.

14. SUBJECT TERMS	15. NUMBER OF PAGES
Engine blades; Ice impact modeling; Root damage analysis; Transient response	12
	16. PRICE CODE: A03

17. SECURITY CLASSIFICATION OF REPORT	18. SECURITY CLASSIFICATION OF THIS PAGE	19. SECURITY CLASSIFICATION OF ABSTRACT	20. LIMITATION OF ABSTRACT
Unclassified	Unclassified	Unclassified	